

U–Pb zircon ages of the host rocks of the Juomasuo Au–Co–Cu deposit, northeastern Finland



PAAVO NIKKOLA^{1*}, IRMELI MÄNTTÄRI² AND O. TAPANI RÄMÖ³

¹ *Nordic Volcanological Center, Institute of Earth Sciences, Sturlugata 7, 101 Reykjavík, Iceland*

² *Geological Survey of Finland, P.O. Box 96, FI-02151 Espoo, Finland*

³ *Department of Geosciences and Geography, Division of Geology and Geochemistry (DiGG), P.O. Box 64, FI-00014 University of Helsinki, Finland*

Abstract

U–Pb zircon single grain dating using the LA-MC-ICP-MS technique was utilized to determine the age of the host rocks of the Juomasuo Au–Co–Cu deposit located in the late Archean Kuusamo supracrustal belt. Even though the dated samples have diverse geochemical signatures that imply felsic volcanic and sedimentary precursors, the U–Pb data revealed heterogeneous detrital zircon populations for all samples. The host rocks are thus considered to belong to reworked sedimentary/volcano-sedimentary sequences. The maximum depositional ages of the samples fall in the 2.75–2.65 Ga age window, and no Paleoproterozoic ages were recovered in the examined zircon grains (151 analytical spots in total). In addition, a younger population (2.65–2.60 Ga) of internally featureless, BSE-pale/CL-dark zircon and zircon domains, was found in the mineralized sequences. These homogenized zircon grains resemble zircon formed in postmagmatic solid-state processes, in which zircon is recrystallized in metamorphic-hydrothermal conditions. This metamorphic-hydrothermal event most probably occurred in the original provenance area of the metasedimentary rocks.

Keywords: U–Pb geochronology, zircon, LA-MC-ICP-MS, Juomasuo, Finland

*Corresponding author (e-mail: paavo@hi.is)

Editorial handling: Jussi S Heinonen (jussi.s.heinonen@helsinki.fi)

1. Introduction

The Paleoproterozoic Kuusamo supracrustal belt is a prominent occurrence of supracrustal rocks in the Central Lapland Greenstone belt in northeastern Finland. The volcano-sedimentary sequences of the belt have been investigated by numerous authors (e.g. Silvennoinen, 1991; Manninen et al., 2001; Räsänen & Huhma, 2001; Laajoki & Huhma, 2006) and, especially, their potential for hosting economic gold deposits has attained attention (Vanhanen, 2001, and references therein). The largest known gold deposit in the Kuusamo supracrustal belt, and also the target of this study, is the Juomasuo Au–Co–Cu deposit.

Based on current understanding, the depositional history of the supracrustal rocks of Finnish Lapland covers a timespan of almost 600 m.y., beginning at ~2450 Ma and ending around ~1880 Ma (Hanski & Huhma, 2005). The deposition of the Kuusamo supracrustal belt occurred between ~2430 Ma and ~2220 Ma. The geochronology of the belt has been troublesome, as primary volcanic strata are rare and delineating depositional ages for the supracrustal sequence has been difficult. Most of the previous datings of the supracrustal rocks of Finnish Lapland depend on U–Pb dating of zircon by the ID-TIMS method. In many of these studies issues have been encountered, related to heterogeneity and discordance of the U–Pb isotopic data (e.g., Hanski et al., 2001). In addition, many studies have acquired ages that are geologically problematic (too old; cf. Hanski et al., 2001). The heterogeneity of zircon populations, strong discordance of the U–Pb data, and anomalously old ages can be explained by metamorphic processes and by incorporation of detrital zircon to the assumed volcanic precursors. In some cases, also erroneous precursor distinctions might be suspected, as determining primary rock types is challenging in the highly tectonized and metamorphosed lithologic units of Lapland.

In this study, the ages of the host rocks of the Juomasuo gold deposit in the Kuusamo supracrustal belt were determined by single grain

U–Pb zircon dating using the LA-MC-ICP-MS method. The size distribution, morphology and texture of the dated zircon grains was analyzed from SEM-images to evaluate whether different zircon age populations would show similar visual characteristics. Geochemical data from the Juomasuo deposit (exploration drillings) and the geochemical classification by Hanes & Schlöglová (2013) enabled us to select the samples to be dated. We focused our sampling efforts to typical rock types of the Juomasuo area with varying precursors, barren and mineralized, as revealed by classification by Hanes & Schlöglová (2013). The need for the study was apparent as the previous geochronological results regarding the area are relatively few and unprecise (cf. Hanski et al., 2001; Räsänen & Vaasjoki, 2001).

2. Kuusamo supracrustal belt and the Juomasuo deposit

The Kuusamo supracrustal belt (Fig. 1) is a large (~2500 km²) volcanic-sedimentary formation on the southern edge of the Central Lapland Greenstone belt, eastern Finland. The belt was deposited unconformably on top of the Archean granite gneiss basement. The depositional time has been delineated between 2.43 Ga and 2.21 Ga (Silvennoinen, 1991; Hanski et al., 2001), although there is some evidence for younger depositional ages of 1.9 Ga from the western parts of the belt (Laajoki & Huhma, 2006). The Kuusamo belt is dominated by deformed, greenschist facies quartzites, siltstones and sericite schists, which are interbedded with mafic lavas and tuffites (Silvennoinen, 1991).

The only Paleoproterozoic age acquired from the supracrustal sequences of the Kuusamo belt is a maximum depositional age of 2405±9 Ma (Fig. 1: location 4) published by Silvennoinen (1991). This age is based on a combined result of three separate samples extracted from acid porphyry clasts in the basal conglomerate, and it has been traditionally considered as the maximum age for the beginning of

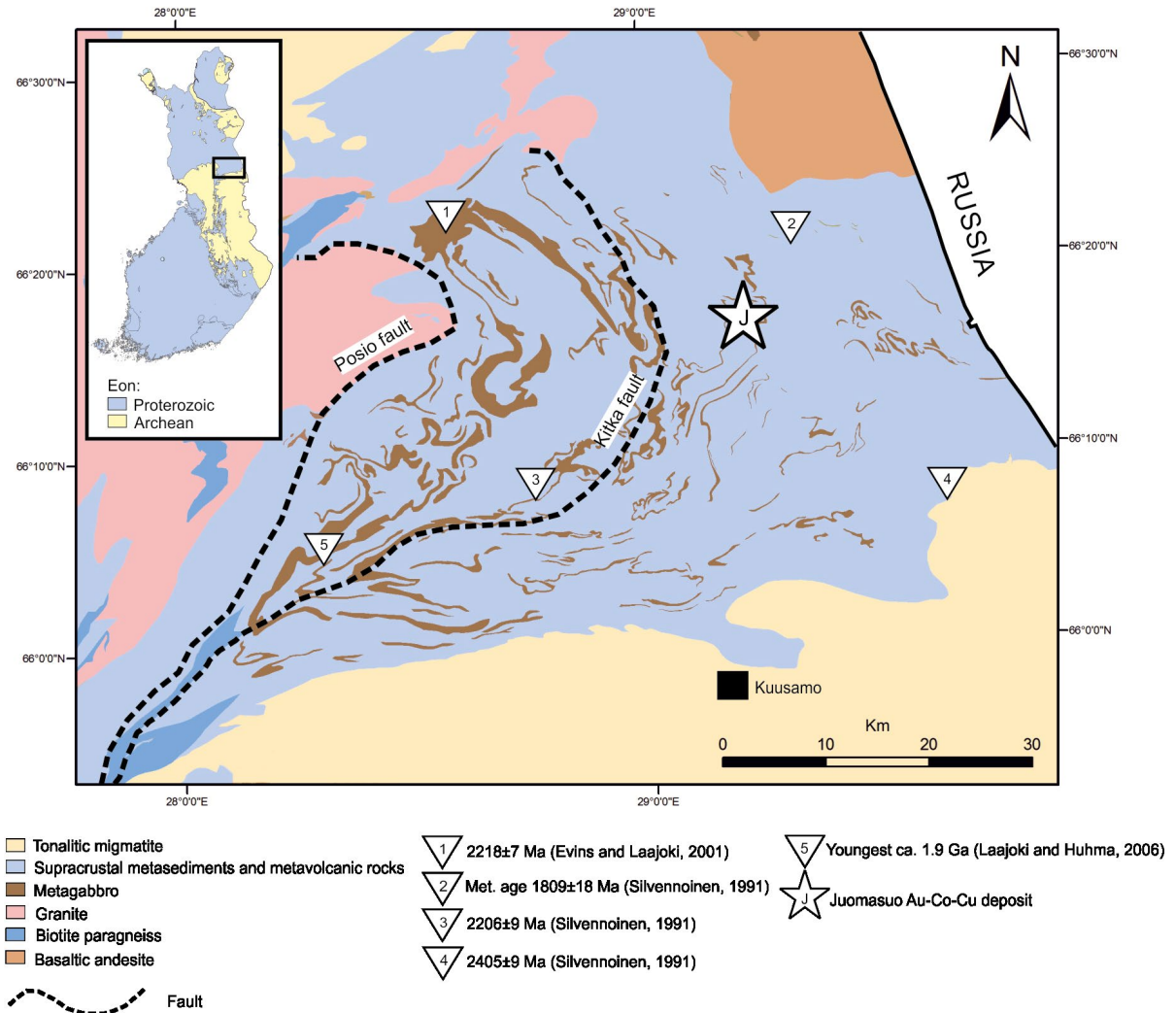


Figure 1. Simplified geological map of the Kuusamo supracrustal belt. Major faults, the Juomasuo Au–Co–Cu deposit, and target areas of notable dating studies (1–5) are marked. Rock types are according to the Bedrock map 1:100 000 of the Geological Survey of Finland (Korsman et al., 1997). Municipality of Kuusamo marked with a square. Inset shows location of the study area relative to Archean and Paleoproterozoic crustal domains in Finland.

the sedimentation in Kuusamo. However, Hanski et al. (2001) proposed that, due to dating problems, a slightly older age of 2432 ± 22 Ma, reported for the quartz porphyries from the Russian side (Buiko et al., 1995), would be preferable.

The minimum age for the deposition of the Kuusamo belt supracrustal rocks is set by the

emplacement of the Tokkalehto metagabbro at 2216 ± 4 Ma (Evins & Laajoki, 2001). This age can also be associated with the emplacement of adjacent mafic sills and dykes that intrude the western parts of the Kuusamo belt, e.g. the metadiabase in the Jäkäläniemi area with an age of 2206 ± 9 Ma (Fig. 1: location 3; Silvennoinen, 1991). An interesting

anomaly in this regard is the Himmerkinlahti member in the western part of the belt, dated by Laajoki & Huhma (2006) (Fig. 1: location 5). U–Pb data from this metaconglomerate–metaquartzite unit imply a maximum depositional age of 1.9 Ga, pointing to deposition after the emplacement of the Tokkalehto metagabbro. The Himmerkinlahti member is poorly exposed and the areal extent of this younger sequence is unknown (Laajoki & Huhma, 2006).

The northern part of the Kuusamo supracrustal belt hosts the target of this study, the Juomasuo Au–Co–Cu deposit (Fig. 1), which is the most economically viable of the ~30 sulfide occurrences in the area. The Juomasuo deposit is an epigenetic shear zone-hosted mineralization, located in the northern end of the Käylä-Konttiahö anticline, approximately 45 km north of the municipality of Kuusamo. The lithostratigraphic position of the deposit is in the upper part of the Sericite Quartzite formation (Silvennoinen, 1972; Vanhanen, 2001). The sequence hosting the main part of the Au–Co–Cu mineralization is composed of quartz-sericite, quartz-chlorite and mixed quartz-sericite chlorite rocks effected by potassic and Fe-rich hydrothermal alteration. In close vicinity of the deposit, the host rocks are intensely albitized, in places also carbonatized and amphibolitized. Ultramafic chlorite-talc-amphibole rocks, probably sills or lavas in origin, are also present. The main economically viable metals of the deposit are gold and cobalt, and the typical ore rock is a sericite or chlorite schist with foliated sulfide dissemination.

The Juomasuo Au–Co–Cu deposit was formed by localized metasomatism caused by circulation of hydrothermal fluids through a shear zone. According to Vanhanen (2001), the mineral paragenesis of the deposit can be explained by four alteration stages: albitization, carbonatization, Mg–Fe-metasomatism and K-metasomatism. The albitization stage was regionally extensive and not restricted to the vicinity of Juomasuo deposit, whereas carbonatization was confined to the Juomasuo shear zone. Carbonatization was followed

by a Mg–Fe-metasomatic phase accompanied by sulfidation as well as Co, and to some degree of Au, mineralization. The main Au enrichment occurred in intense K-metasomatism at the end of the alteration sequence. This took place simultaneously to sericification and silicification in the core part of the deposit.

Because of the extensive alteration surrounding the Juomasuo deposit, the precursor rock can rarely be distinguished in the field. To overcome this problem, Hanes & Schläglóvá (2013) used the ratios of elements that are immobile during hydrothermal alteration (Zr, Nb, Hf, Ta, REE, Ti and Al) to determine primary rock types. Especially the Zr/TiO₂ and Nb/Y ratios were deployed as they were inferred to be useful in determining precursor rock types. Juomasuo host rock precursors were determined as mainly metasedimentary; although felsic and mafic volcanic rocks are also commonly found interlayered in the sedimentary sequences.

Although the mineralization is dominantly structurally controlled by a NW–SE trending shear zone (Vanhanen, 2001), Hanes & Schläglóvá (2013) argued that it also has a strata bound character to a distinct horizon of volcanic and sedimentary rocks. This horizon is gently folded and enveloped by rocks with ultramafic precursors (Hanes & Schläglóvá, 2013). The highest gold grades are found in pencil-shaped ore shoots in the fold hinges of the ore body. The total resources of the deposit, based on March 2014 JORG complied figures, are 2 371 000 tons grading 4.6 g/t gold for 347,000 ounces and 5 040 000 tons grading 0.12 % cobalt for 5 900 cobalt tonnes (Dragon Mining Ltd, 2014).

The age of the Juomasuo Au–Co–Cu mineralization is unknown. There is, however, a U–Pb age of approximately 1830 Ma from a pyrrhotite with brannerite inclusions from the nearby Hangaslampi deposit (Mänttári, 1995). Most probably this records the timing of subsequent sulfide mobilization.

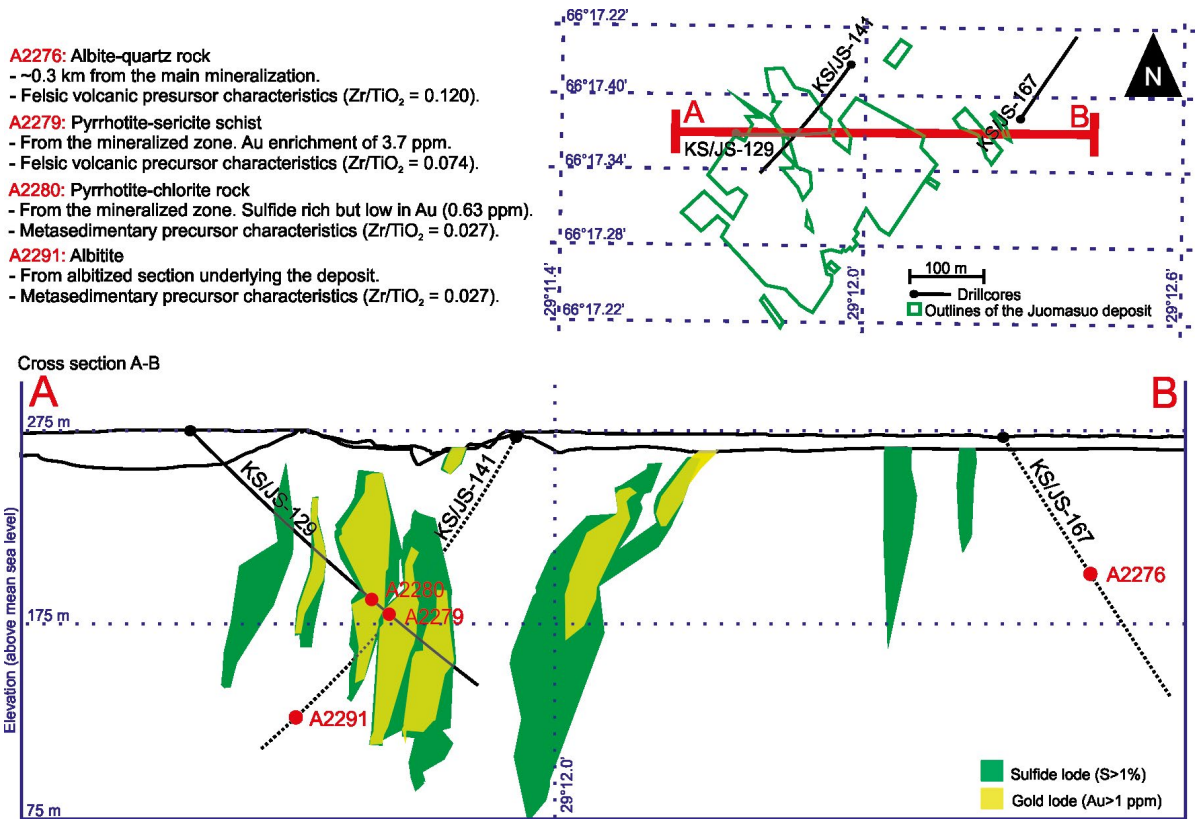


Figure 2. Position of the samples examined in this study relative to a depth profile of the Juomasuo deposit. Upper image shows the outline of the Juomasuo deposit projected to the topographic surface, position of cross section A-B, and drilling locations. Lower image depicts cross section A-B with the sample locations and mineralized zones. Only the drill hole KS/JS-129 is on the cross section, whereas the drill holes KS/JS-141 and KS/JS-167, and their corresponding sample locations A2291 and A2267, represent projections to the cross section surface. Coordinates in WGS 84.

3. Samples

The rocks dated in this study were acquired from the comprehensive drill core archives of Dragon Mining Ltd and were chosen to represent the most typical rock types of the Juomasuo area, both mineralized and barren. The samples were derived from pulps made from split drill cores varying in length from 1.00 to 2.25 m. The Zr/TiO_2 ratio, used for the Juomasuo deposit by Hanes & Schlöglóvá (2013), was used to distinguish the rock precursors and in sample selection. In the end, four samples yielded enough zircon (> 50 grains each).

Location of the examined samples in relation to the mineralization is shown in Fig. 2. Two of

the samples are from the gold mineralized zone of the deposit: pyrrhotite-sericite schist A2279 and a pyrrhotite-chlorite rock A2280. Both are from the same drill core that cuts the main mineralization at an approximate depth of 90 m below ground-level (Fig 2). Pyrrhotite-sericite schist A2279 has 3.7 ppm gold, whereas the gold content in pyrrhotite-chlorite rock A2280 is only 0.63 ppm, although the latter is strongly enriched in sulfides (pyrrhotite and pyrite). Sample A2279 shows geochemical characteristics of a felsic volcanic precursor ($Zr/TiO_2 = 0.074$), whereas sample A2280 could be metasedimentary in origin ($Zr/TiO_2 = 0.027$). Because of the intense alteration and foliated, primary features of the precursor rock have been erased.

Samples A2276 and A2291 are barren and free from the imprint of the Juomasuo mineralization. A2276 is a foliated albite-quartz rock with high a Zr/TiO_2 value of 0.120 that implies a felsic volcanic precursor, whereas A2291 is a brecciated massive albitite with metasedimentary precursor characteristics ($Zr/TiO_2 = 0.027$). A2291 is from an intensively albitized block that underlies the main mineralization at a depth of 150 m. A2267 was taken about 300 meters NW from the deposit from a depth of ~75 m (Fig. 2). Zircon in A2267 seems to be enriched to a horizon clearly visible in thin section. This might imply sedimentary reworking and gravitational sorting of the sediment precursor.

4. Methods

4.1. Sample preparation

The sample pulps were powdered using a swing mill (run time ~20 s) and fine-grained material from the mill was washed away. Separation of zircon from dry powder was made using heavy liquids, i.e. methylene iodide ($\rho = 3.3$ g/ml) and Clerici solution ($\rho = 3.8$ g/ml). Magnetic minerals were separated using a Frantz magnetic separator. Every zircon from the resulting heavy fraction was hand-picked under a binocular microscope. The zircon grains were then casted in epoxy resin, which was sectioned in half and polished. Finally, the epoxy molds containing the zircon were imaged with scanning electron microscope (SEM) using cathodoluminescence (CL) and backscatter electron (BSE) detectors.

4.2. Zircon size evaluation

All SEM images of zircon were studied using ImageJ image analysis software (Abramoff, 2004) to solve the zircon grain-size distribution and to examine the morphology. For every sample, CL and BSE images were combined to a single file from which zircon were hand selected using a GIMP image manipulation software. The images

were then transformed to binary-images and the zircon size and shape was quantified with ImageJ. A minimum Feret's diameter, parameter widely used in morphometric analysis, was used to determine the zircon size. This measure (sometimes referred as minimal Feret's diameter, Least Feret's diameter, Feret's width or minimum caliber) corresponds to the minimum distance of two parallel tangents at opposing borders of the mineral. Minimum Feret's diameter was applied, as it is quite unsusceptible to the error caused by the orientation of the section angle and the size information attained with it resembles traditional sieve analysis.

Visual zircon size evaluation can be biased by careless polishing of the zircon bearing epoxy mounts. During the sample preparation, zircon grains are laid to an epoxy which is polished so that the grains are exposed on the epoxy surface. Although the method aims to a perfect, even cross-sections of the grains, some grains can be left only partly surfaced or almost completely polished out. This effect produces smaller minimum Feret's numbers than the actual grain dimensions, and thus the mean grain size will always be underestimated by some degree. This effect can be minimized by careful preparation, but the potential operator induced bias remains. However, the method gives a quantitative numerical value of the grain size and distinct grain size populations within a single sample can be detected if present.

4.3. U–Pb dating

U–Pb dating was performed in two separate sessions in the Finland Geoscience Laboratory (SGL), Espoo, in February 2014. A new wave Analyte G2 193 nm laser microprobe was used in static ablation mode with a beam diameter of 20 μm , pulse frequency of 5 Hz and beam energy density of 0.83 J/cm³. The 20 μm beam diameter hampered the analysis of smallest zircons and zircon domains. Every U–Pb measurement included 20 seconds of background measurement, which was followed by 70 seconds of ablation with a stationary laser beam. Secondary electron multipliers were used to

Table 1. Classification criteria used to distinguish the analyzed zircon domains of different origin.

Measurement classes	
1	Zoned zircon domain, which should give an undisturbed magmatic age.
2	Inherited core domain with visible compositional zoning; possible evidence for crustal recycling.
3	BSE-pale/Cl-dark texturally homogeneous zircon domain; most probably yielding a homogenization age.
4	BSE-dark homogenous/Cl-bright zoned or rather homogeneous zircon domain; most probably metamorphic in origin.

measure the masses 204, 206 and 207; the mass 238 was measured using a Faraday collector.

The raw data were corrected for background, laser induced elemental fractionation, mass discrimination, and drift in ion counter gains, and reduced to U–Pb ratios by calibrating to concordant reference zircon of known age, using the protocols of Andersen et al. (2004) and Jackson et al. (2004). Reference samples GJ-01 (609±1 Ma; Belousova et al., 2006) and A1772 (2711±3 Ma; Huhma et al., 2012) were used for data reduction. In addition, the sample A382 (1877±2 Ma; Huhma et al., 2012) was measured as a reference sample to check the calibration. Age related common lead (Stacey & Kramers, 1975) correction was used if the analysis showed common lead contents above detection limits. An interactive Excel spreadsheet program written by Professor Tom Andersen, University of Oslo (cf. Rosa et al., 2009) was used for data reduction.

The U–Pb isotopic data was processed using the Isoplot Excel program (Ludwig, 2003). Only the concordant or slightly discordant (central discordance < 8%) U–Pb data, where the ablation spot remained inside one zircon phase/domain, were qualified. All ages and error bars in figures are presented with 2σ errors (without decay constant errors). Individual zircon ages are classified based on the appearance of the measured spot, and by using the partitioning shown in Table 1. This was done to distinguish zircon ages of different origin (i.e. magmatic crystallization ages, metamorphic ages and inherited ages). Many of the zircon domains of interest were too small, cracked, or altered, to be measured using the applied 20 μm analysis spot size.

5. Results

5.1. Zircon grain size and morphology

The samples A2276 and A2279, with high Zr/TiO₂ and thus a felsic volcanic geochemical signature have, on average, larger zircon grains than samples A2280 and A2291 with metasedimentary affinity (Fig. 3). The average zircon size in A2276 is 67 μm and in A2279 it is 70 μm, whereas the average grain sizes are only 56 μm and 49 μm for samples A2280 and A2291 respectively. All samples show a unimodal distribution somewhat skewed towards finer crystal size. The greatest variance in grain size is the found from sample A2279 and the clearly lowest in sample A2291. The zircon morphology is overall rounded with many of the grains having an ellipsoidal shape. Only few of the zircon are euhedral or subhedral, and primary magmatic morphologies, e.g. pyramid shaped crystal ends, are scarce. Some mounted grains were clearly shards or pieces of originally whole zircon potentially broken during sample preparation. We did not find any link between the zircon age and the morphology of the magmatic zircon, and there was no clear quantifiable difference in zircon morphology between the samples. However, texturally homogenous zircon and zircon domains from the mineralized horizon (samples A2279 and A2280) were found to have younger ages compared to other zircon analyzed.

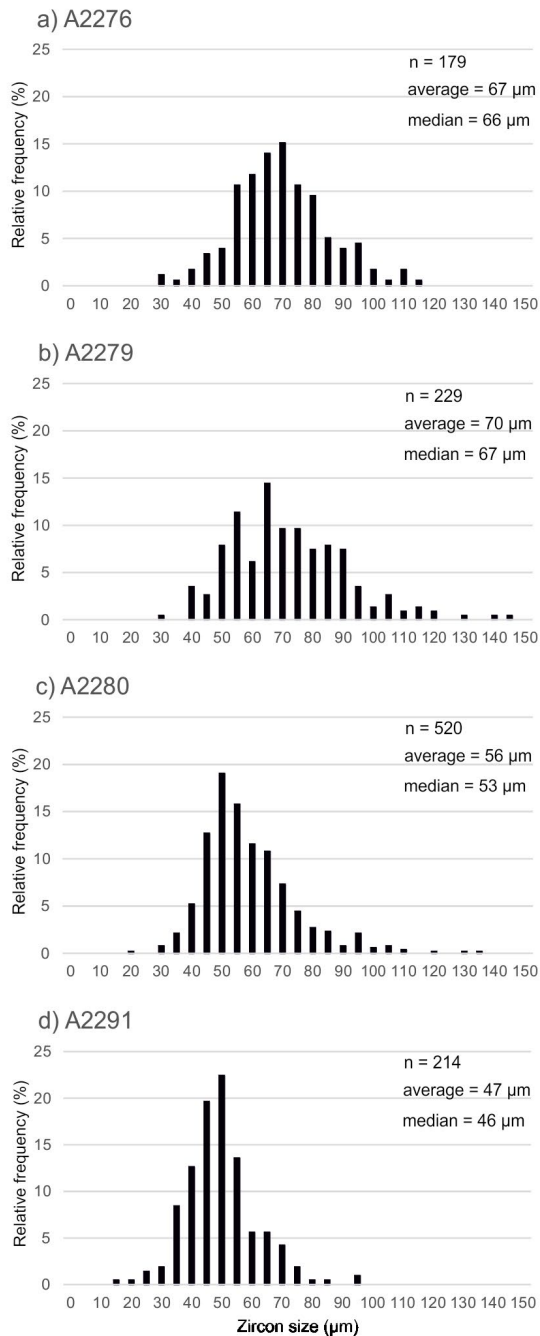


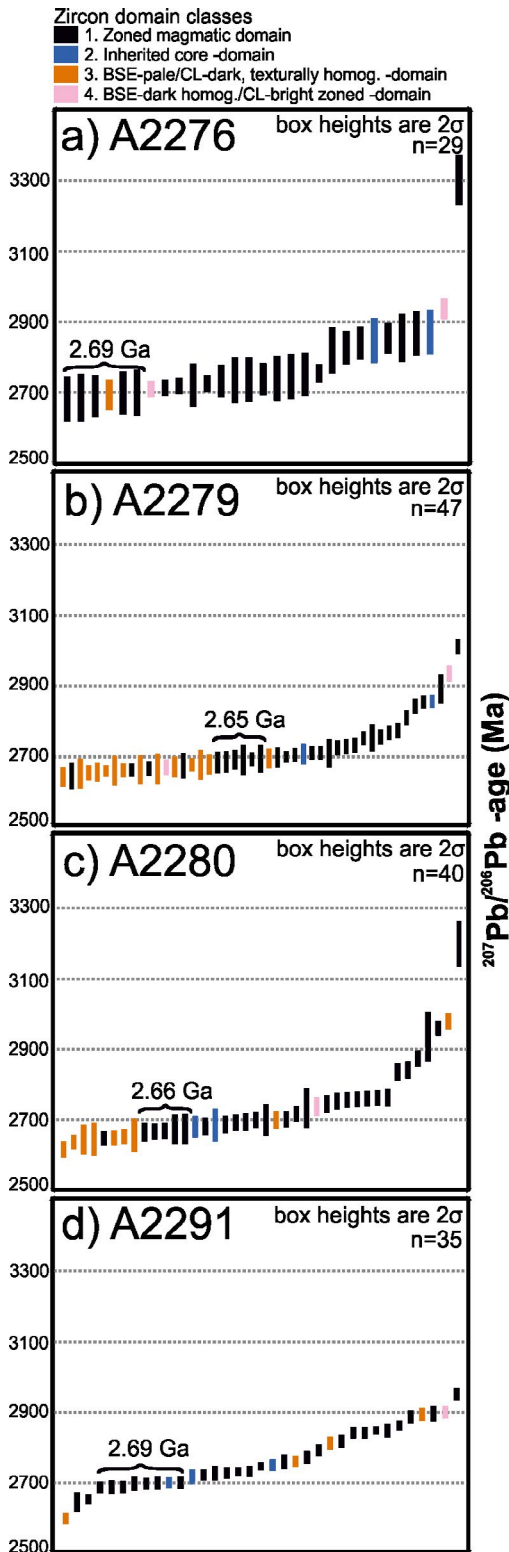
Figure 3. Size distribution of zircon grains acquired from the dated samples a) A2276, b) A2279, c) A2280 and d) A2291.

5.2. U–Pb ages

From the 1142 zircon crystals separated from the host rocks of the Juomasuo deposit, 151 zircon domains were successfully dated. The U–Pb data are concordant, and only a few measurements had to be rejected (Table 2). However, as individual zircon crystals and zircon domains were generally small, only a limited amount of the grains could be dated per sample (Table 2). The results show a wide variety of magmatic detrital zircon ages between 2.90 Ga and 2.65 Ga with some isolated ages in excess of 2.90 Ga (Fig. 4). A summary of the age results is shown in Figure 4 and Table 2, and the complete U–Pb data set is provided in Electronic Appendix A.

Sample A2276, from the barren rocks surrounding the deposit, has wide scatter in $^{207}\text{Pb}/^{206}\text{Pb}$ ages regardless its affinity to felsic volcanic precursor (Fig. 4a). The majority of the $^{207}\text{Pb}/^{206}\text{Pb}$ ages plot between 2.73–2.70 Ga and ~2.85 Ga ages are also abundant. The maximum depositional age of the sample can be constrained by the age of the five youngest zircon domains with magmatic texture to 2694 ± 27 Ma (MSWD=0.07; Fig. 4a)

The other barren sample, A2291, with a sedimentary precursor affinity, is similar to sample A2276 in terms of the $^{207}\text{Pb}/^{206}\text{Pb}$ data. However, the greater analytical precision allows distinction of more evenly graded scatter of ages. $^{207}\text{Pb}/^{206}\text{Pb}$ ages of 2.69 Ga and 2.71 Ga are common. The maximum depositional age 2694 ± 6 Ma for A2291 is calculate using seven zircon domains with internal magmatic texture forming the youngest congruent age group (MSWD=0.57; Fig. 4d). The young ages from sample A2291 (A2291_15a = 2602 ± 14 Ma, A2291_21a = 2647 ± 26 Ma, A2291_34a = 2654 ± 12), are considered outliers, and maximum depositional age cannot be interpreted based on these data points alone. More analyses of such young zircon might, however, justify a younger maximum depositional age (i.e. ~2.66–2.65 Ga).



Sample A2279, from the mineralized horizon of Juomasuo deposit and with a felsic volcanic geochemical affinity, is characterized by texturally homogenous zircon domains (Fig. 5a, b, c and d) and by overall younger $^{207}\text{Pb}/^{206}\text{Pb}$ ages compared to the barren samples (Fig. 4). The majority of the $^{207}\text{Pb}/^{206}\text{Pb}$ data plot between 2.68 Ga and 2.60 Ga three grains have ages around 2.70 Ga, and the remaining $^{207}\text{Pb}/^{206}\text{Pb}$ ages scatter evenly between 3.0 Ga and 2.72 Ga (Fig. 4b). Zircon domains younger than 2.70 Ga are dominantly texturally homogenous.

The thoroughly mineralized sample A2280 with sedimentary affinity has younger $^{207}\text{Pb}/^{206}\text{Pb}$ ages than the barren samples, and alike A2279, it is characterized by texturally homogenous zircon domains. Half of the $^{207}\text{Pb}/^{206}\text{Pb}$ ages fall within the 2.70–2.60 Ga time frame, many have ages of 2.7 Ga, and there is a somewhat defined population of zircon ages of 2.75–2.72 Ga (Fig. 4c). The very similar U–Pb zircon age characteristics of A2279 and A2280 might imply genetic similarity between the samples regardless their different precursor distinctions.

In both samples from the mineralized horizon (A2279 and A2280), homogenized zircon domains form the youngest age group, with ages between 2.65 and 2.60 Ga. If the zircon were homogenized predepositionally, the recrystallization age 2.60 Ga is also the maximum depositional age for the mineralized samples. However, if zircon homogenization occurred after deposition,

Figure 4. Illustration of the dating results ($^{207}\text{Pb}/^{206}\text{Pb}$ ages of individual zircon spots) of the four samples examined: a) albite-quartz rock (felsic volcanic precursor) A2276, 29 spots; b) pyrrhotite-sericite schist (felsic volcanic precursor) A2279, 47 spots; c) pyrrhotite-chlorite rock (metasedimentary precursor) A2280, 40 spots; d) albite (metasedimentary precursor) A2291, 35 spots. The data spots are color-coded based on the classification shown in Table 1. Magmatic zircons that yield maximum depositional ages are indicated.

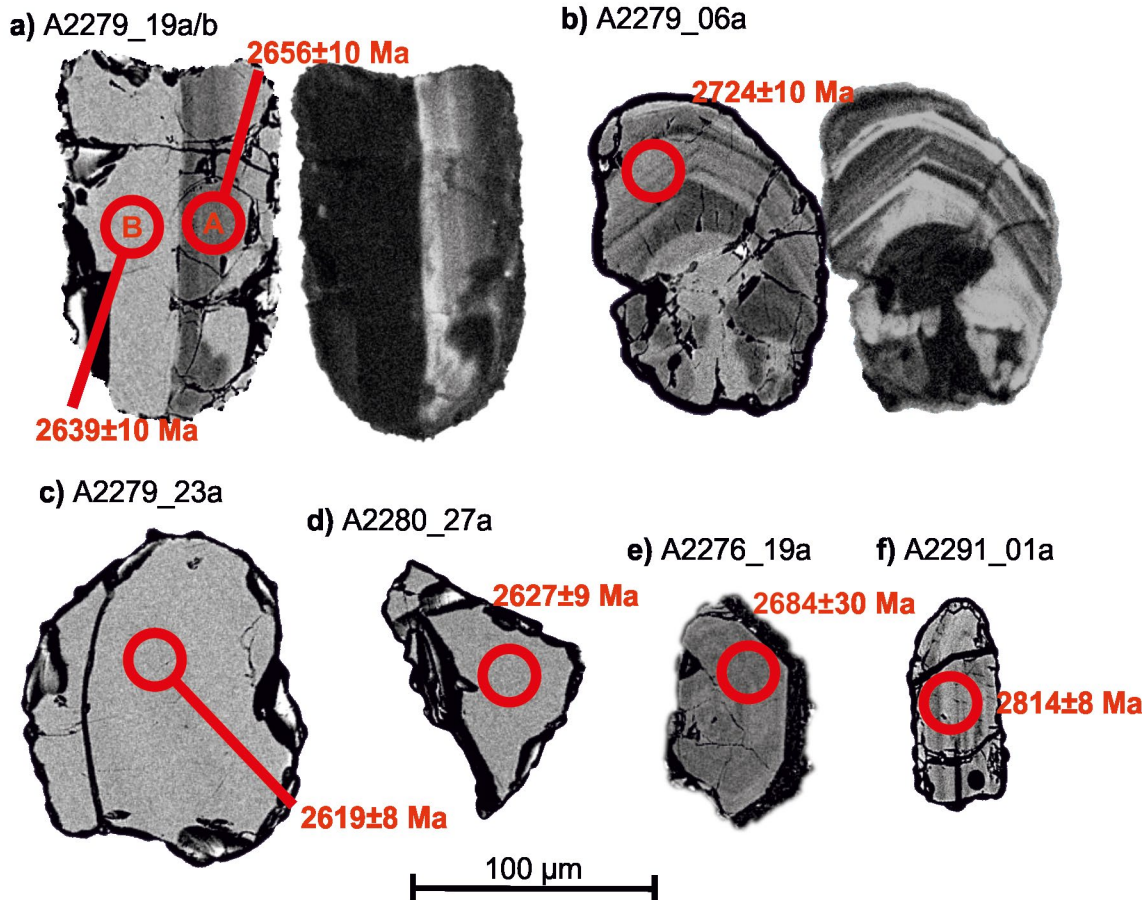


Figure 5. Examples of analyzed zircon grains with $^{207}\text{Pb}/^{206}\text{Pb}$ ages of analytical spots indicated. a) Sample A2279, two spots analyzed (A2279_19a and A2279_19b). BSE-image on the left, CL-image on the right. Measurement “a” is from blurred magmatic domain, and measurement “b” from texturally homogenized domain. b) Sample A2279, magmatic zircon (analytical spot A2279_06a) with a recrystallized homogenous core surrounded by CL-bright recrystallization front. BSE-image on the left, CL-image on the right. c) Sample A2279, texturally homogenized zircon (analytical spot A2279_23a). BSE-image. d) Sample A2280, texturally homogenized zircon fragment (analytical spot A2280_27a). BSE-image. e) Sample A2276, magmatic zircon (analytical spot A2276_19a). BSE-image. f) Sample A2291, magmatic zircon (analytical spot A2291_01a). BSE-image.

deposition of A2279 probably took place between recrystallization at 2.60 Ga and maximum sedimentation age of 2.65 Ga (mean age: 2653 ± 12 Ma, MSWD=0.10; Fig. 4b). The same would apply to sample A2280, for which deposition should

have occurred between 2.60 Ga and maximum depositional age 2.66 Ga (mean age: 2658 ± 11 Ma, MSWD=0.05, $n=5$; Fig. 4c). Pre-depositional zircon homogenization is considered as a more probable option (see below).

Table 2. Summary of the sample characteristics and the U–Pb dating results.

Sample	Zircon yield	Petrographic description	Zr/TiO ₂	Max. dep. age (Ga)	Age peaks (Ga)	Recryst. age (Ga)
A2276 Albite–quartz rock (geochemically felsic volcanic rock)	179 zircon separated, 34 zircon dated, and 5 zircon ages rejected.	Mildly foliated and intensively albitized rock. Main minerals: Qz, Ab, Bt, Ser. Accessory minerals: Zr, Cb.	0.120	2.69	2.72 2.85	-
A2279 Pyrrhotite–sericite schist (geochemically felsic volcanic rock)	229 zircon separated, 49 zircon dated, and 2 zircon ages rejected.	Sericite schist with abundant pyrrhotite. Main minerals: Ser, Po, Ab, Qz. Accessory minerals: Bt, Zr, Py, Ccp.	0.074	2.60 or 2.65*	2.63 2.65	2.60
A2280 Pyrrhotite–chlorite rock (geochemically metasedimentary rock)	520 zircon separated, 44 zircon dated, and 4 zircon ages rejected.	Foliated chlorite and pyrrhotite rich rock. Main minerals: Chl, Qz, Ser, Ab, Po, Mag. Accessory minerals: Zr, Py.	0.027	2.60 or 2.66*	2.63 2.68 2.74	2.60
A2291 Albitite (geochemically metasedimentary rock)	214 zircon separated, 50 zircon dated, 15 zircon ages rejected.	Massive brecciated albitite. Main minerals: Ab, Qz, Cb. Accessory minerals: Bt, Ser, Zr.	0.027	2.69	2.70 2.73 2.85	-

*This age applies if zircon recrystallization is post-depositional.

Abbreviations used: Max. dep. age= maximum depositional age, Recryst. age= recrystallization age, Ab= albite, Bt= biotite, Cb= carbonate mineral, Ccp= chalcopyrite, Chl= chlorite, Mag= magnetite, Po= pyrrhotite, Py= pyrite, Qz= quartz, Ser= sericite, Zr= zircon.

6. Discussion

The U–Pb data acquired for the country rocks of the Juomasuo deposit imply the following:

(1) A sedimentary origin is suggested for the supposed felsic metavolcanic rocks because of the relatively large spread of Archean ages derived from the samples and the apparent similarity in ²⁰⁷Pb/²⁰⁶Pb age distribution between the felsic metavolcanic and metasedimentary samples.

(2) At 2.60 Ga, a metamorphic-hydrothermal event caused the homogenization of the zircon/zircon domains in samples derived from the mineralized sequences of the Juomasuo deposit.

(3) There are no signs of Paleoproterozoic volcanism in the studied sequences in the Juomasuo area, as all the derived ages are Archean.

In view of the large age variability of the zircon derived from the (geochemically) volcanic samples from the Juomasuo deposit, it is improbable that the rock precursor would have been a tuff, lava flow, or any other primary felsic volcanic rock. The precursor of the mineralized horizon of the Juomasuo deposit (samples A2279 and A2280) could have been a lithic arenite with volcanic or plutonic fragments. The geochemical variation from felsic volcanic to sedimentary precursors (Hanes & Schlöglová, 2013) could actually be a reflection of the grain size, sorting and purity variation inside the sedimentary sequence, i.e. the layers with plentiful igneous lithic fragments would show as geochemically felsic volcanic horizons.

The appearance of the completely and partly texturally homogenized zircon domains in the rock

types of the mineralized sequence (samples A2279 and A2280) is analogous to zircon studied by Schaltegger et al. (1999), Hoskin & Black (2000), and Möller et al. (2002). These domains have low CL–intensity and they are internally featureless (homogeneous). Occasionally the homogeneous domains are surrounded by CL–bright featureless recrystallization fronts (Fig. 5a and b; Fig. 2 in Hoskin & Black, 2000; Möller et al. 2002). We interpret these zircon domains to have been formed by a solid state recrystallization of the protolith zircon in a high grade metamorphism (cf. Hoskin & Black, 2000).

Even though the homogenized zircon domains yielded ages between 2.65 and 2.60 Ga, 2.60 Ga is the probable age of homogenization. This was warranted, as the homogenized domains yielding younger ages were more robust compared to the older ones, which are probably biased by incomplete homogenization which results to ‘mixed’ U–Pb ages between the magmatic and metamorphic events (cf. Hoskin & Schaltegger, 2003).

Only four age pairs, in which the other age is from a domain with magmatic texture and the other from a homogenized domain of the same zircon (e.g. Fig. 5a), were successfully measured. For these, the texturally magmatic zircon domains belong to a 2.67–2.66 Ga population, and the age of homogenized domains is 2.65–2.60 Ga. This implies pre-depositional recrystallization/homogenization, because all magmatic zircon that has experienced homogenization belong to a one distinct age group. In addition, metamorphic zircon domains formed by solid state recrystallization have been earlier documented mainly from granulite–facies rocks (Hoskin & Schaltegger, 2003), whereas the Juomasuo host rocks have only experienced greenschist to lower amphibolite facies metamorphism (Vanhanen, 2001). Because of all this, we consider the homogenized zircon having been inherited from a pre-depositional source. Homogenization of zircon thus occurred in the plutonic/metamorphic provenance of the sedimentary rock.

As the young recrystallized/homogenized zircon were only found from the mineralized samples, this could indicate a distinct source region for the mineralized sequence. However, ages from only two samples taken relatively close to each other (Fig. 2) cannot be generalized for the whole deposit, and further studies are needed to validate this hypothesis. Furthermore, a distinct population of detrital zircon ages in a sedimentary sequence does not automatically necessitate a change in source region, as variation in the erosional level and relief of a single zircon source can impose changes to the detrital zircon populations derived. Only a slight change in the local sedimentary environment might have led to the accumulation of the homogenized zircon (of inferred high-grade metamorphic origin) to the sedimentary horizon currently hosting the Au–Co–Cu enriched rocks of the Juomasuo deposit.

The homogenized zircon domains infer a high-grade metamorphic terrain in the provenance of the Juomasuo metasedimentary rocks and, taking into account the nonconformable position of the Kuusamo belt relative to the Archean Kuhmo complex (Silvennoinen, 1991), the mid-crustal Archean rock suites also within the more distal segments of the Finnish part of the Archean Karelia Province can be considered as potential protoliths of the Juomasuo metasedimentary rocks. The majority of the Juomasuo magmatic zircon ages plot to a time frame between 2.75 Ga and 2.65 Ga, although some older ages up to 3.3 Ga are present. Within the Finnish part of the Archean Karelia Province, the most fitting currently exposed rock suites for these detrital zircon would be the granodiorite–granite–monzogranites (GGM), 2.73–2.66 Ga (Käpyaho et al., 2006); quartz diorite–quartz monzodiorites (QQ), c. 2.70 Ga; or sanukitoids (high Mg–granitoids), 2.74–2.72 Ga (Heilimo et al., 2012). The mid-crustal TTG (tonalite–trondhjemite–granodiorite) rocks, which occupy the majority of the Archean of the Fennoscandian shield, are generally older than 2.72 Ga (Hölttä et al., 2012), and thus their age do not coincide with the peak in Juomasuo zircon ages. Most of the detrital zircon found in this study could originate

from now eroded plutonic and supracrustal rocks resembling the same magmatic-metamorphic event that formed the GGM, QQ and sanukitoid granitoids. In turn, the zircon older than 2.72 Ga could be directly related to TTG-type magmatism, although interestingly, the Juomasuo rocks have a well-defined population of c. 2.85 Ga zircon, and there are no TTGs of this age in the Finnish part of the Archean Karelian Province (cf. Fig. 21 in Hölttä et al., 2012). Signs of felsic magmatism of this age can however be found from the Archean greenstone belts of eastern Finland (e.g. Lehtonen & Käpyaho, 2016).

Based on current understanding, the Kuusamo supracrustal belt was deposited between 2.43 Ga and 2.21 Ga (Silvennoinen, 1991; Hanski et al., 2001). The absence of ages of syndepositional volcanism is puzzling. Although it is not uncommon for sedimentary rocks to be constituted from material even hundreds of millions of years older than the age of the deposition (Fedó et al., 2003, and references therein), one would expect some primary felsic volcanic horizons to be interbedded within the Kuusamo metasedimentary sequence. The area has been volcanologically active during the deposition, as clearly demonstrated by the abundant mafic volcanic rocks (e.g. pillow basalts; Silvennoinen, 1991).

7. Concluding remarks

Our data from the host rocks of the Juomasuo gold deposit fail to reveal evidence of Paleoproterozoic volcanism, and the wide range of ages acquired from the four samples examined implies a sedimentary origin for the studied rocks. The samples from the mineralized sequence of the Juomasuo deposit have a population of homogenized zircon formed by solid-state recrystallization of protolith igneous zircon. This finding implies a metamorphic–

hydrothermal event around 2.60 Ga in the source area of the Juomasuo sedimentary sequence. This is compatible with the fact that only a part of the population of 2.67–2.66 Ga magmatic zircon was affected by the recrystallization and the local metamorphic conditions were not potent enough to produce the observed zircon textures subsequent to deposition. Distinct provenance of zircon in the mineralized horizon might also imply a different source region for the Au–Co–Cu enriched sedimentary rocks in comparison to the non-mineralized sedimentary rocks surrounding the deposit.

Acknowledgements

This paper is a spin-off of the M.Sc. thesis of the first author at the University of Helsinki (Nikkola, 2014). The work was conducted as collaboration between Geological Survey of Finland, Dragon Mining Ltd and the University of Helsinki. Special credit is given to the personnel of Research Laboratory of Geological Survey of Finland and the Finland Isotope Geosciences Laboratory (SGL, a joint venture between the GTK and the geoscience universities of Finland). Comments by the journal reviewers (Docent Tapio Halkoaho, Dr. Elina Lehtonen) and the Editor-in-Chief (Docent Jussi Heinonen) improved the manuscript. The current stakeholder of the Juomasuo deposit, Nero Projects Australia Pty Ltd, is acknowledged for the licence to publish the data reported in this paper.

Supplementary data

Electronic Appendix A for this article is available via Bulletin of the Geological Society of Finland web page.

References

- Abramoff, M.D., Paulo, J.M. & Sunanda, R.J., 2004. Image Processing with ImageJ. *Biophotonics international* 11, 36–42.
- Andersen, T., Griffin, W.L., Jackson, S.E. & Knudsen, T.L., 2004. Mid-Proterozoic magmatic arc evolution at the southwest margin of the Baltic Shield. *Lithos* 73, 289–318.
<https://doi.org/10.1016/j.lithos.2003.12.011>
- Belousova, E.A., Griffin, W.L. & O'Reilly, S.Y., 2006. Zircon crystal morphology, trace element signatures and Hf isotope composition as a tool for petrogenetic modelling: examples from Eastern Australian granitoids. *Journal of Petrology* 47, 329–353.
<https://doi.org/10.1093/petrology/egi077>
- Buiko, A., Levchenkov, O., Turchenko, S. & Drubetskiy, E., 1995. Geology and isotopic dating of the early Proterozoic Sumian-Sariolian Complex in northern Karelia (Paanajärvi-Tsipringa structure). *Stratigraphy, Geological Correlation* 3 (4), 16–30. (In Russian)
- Dragon Mining Ltd, 2014. ASX announcement, 18 March 2014: Resource updates lift Kuusamo ounces. March 2014, 64p.
- Evins, P.M. & Laajoki, K., 2001. Age of the Tokkalehto metagabbro and its significance to the lithostratigraphy of the early Proterozoic Kuusamo supracrustal belt, Northern Finland. *Bulletin of the Geological Society of Finland* 73, 5–15.
- Fedo, C.M., Sircombe, K.N., Rainbird, R.H., Hanchar, H.M. & Hoskin, P.W.O. 2003. Detrital zircon analysis of the sedimentary record. In: Hanchar, J.M. & Hoskin, P.W.O. (eds.), *Zircon. Reviews in Mineralogy and Geochemistry* 53, 277–303.
<https://doi.org/10.2113/0530277>
- Hanes, R. & Schöglövá, K., 2013. Lithogeochemistry of the Juomasuo and Hangaslampi deposits, Kuusamo, Finland. Internal report, Dragon Mining Sweden AB. 59 p.
- Hanski, E., Huhma, H. & Vaasjoki, M., 2001. Geochronology of northern Finland: a summary and discussion. In: Vaasjoki, M. (ed.), *Radiometric age determinations from Finnish Lapland and their bearing on the timing of Precambrian volcano-sedimentary sequences*. Geological Survey of Finland 33, 255–279.
- Hanski, E. & Huhma, H., 2005. Central Lapland greenstone belt. In: Lehtinen, M., Nurmi, P.A. & Rämö, O.T. (eds.), *Precambrian Geology of Finland – Key to the Evolution of the Fennoscandian Shield*. Elsevier B.V., Amsterdam, pp. 139–194.
- Heilimo, E., Halla, J. & Mikkola, P., 2012. Overview of Neoarchaean sanukitoid series in the Karelia Province, eastern Finland. Geological Survey of Finland, Special Paper 54, 214–225.
- Hölttä, P., Heilimo, E., Huhma, H., Kontinen, A., Mertanen, S., Mikkola, P., Paavola, J., Peltonen, P., Semprich, J., Slabunov, A. & Sorjonen-Ward, P., 2012. The Archaean of the Karelia Province in Finland. Geological Survey of Finland, Special Paper 54, 21–73.
- Hoskin, P.W.O. & Black, L.P., 2000. Metamorphic zircon formation by solid-state recrystallization of protolith igneous zircon. *Journal of Metamorphic Geology* 18, 423–439.
<https://doi.org/10.1046/j.1525-1314.2000.00266.x>
- Hoskin, P.W.O. & Schaltegger U., 2003. The composition of Zircon and Igneous and Metamorphic Petrogenesis. In: Hanchar, J.M. & Hoskin, P.W.O. (eds.), *Zircon. Reviews in Mineralogy and Geochemistry* 53, pp. 469–499.
<https://doi.org/10.2113/0530027>
- Huhma, H., Mänttari, I., Peltonen, P., Kontinen, A., Halkoaho, T., Hanski, E., Hokkanen, T., Hölttä, P., Juopperi, H., Konnunaho, J., Layahe, Y., Luukkonen, E., Pietikäinen, K., Pulkkinen, A., Sorjonen-Ward, P., Vaasjoki, M. & Whitehouse, M., 2012. The age of the Archaean greenstone belts in Finland. Geological Survey of Finland, Special Paper 54, 74–175.
- Jackson, S.E., Pearson, N.J., Griffin, W.L. & Belousova, E. A., 2004. The application of laser ablation-inductively coupled plasma-mass spectrometry to in situ U–Pb zircon geochronology. *Chemical Geology* 211, 47–69.
- Käpyaho, A., Mänttari, I. & Huhma, H. 2006. Growth of Archaean crust in the Kuhmo district, eastern Finland: U–Pb and Sm–Nd isotope constraints on plutonic rocks. *Precambrian Research* 146, 95–119.
<https://doi.org/10.1016/j.precamres.2006.01.006>
- Korsman, K., Koistinen, T., Kohonen, J., Wennerström, M., Ekdahl, E., Honkamo, M., Idman, H. & Pekkala, Y. (eds.), 1997. Bedrock map of Finland 1:1 000 000. Geological Survey of Finland.
- Laajoki, K. & Huhma, H., 2006. Detrital zircon dating of the Palaeoproterozoic Himmerkinlahti Member, Posio, Northern Finland; Lithostratigraphic implications. *Bulletin of the Geological Society of Finland* 78, 177–182.
- Lehtonen, E. & Käpyaho, A., 2016. A small Archaean belt – diverse age ensemble: A U–Pb study of the Tipasjärvi greenstone belt, Karelia Province, central Fennoscandian Shield, Finland. *Lithos* 246–247, 31–47.
<https://doi.org/10.1016/j.lithos.2015.11.008>
- Ludwig, K.R., 2003. *Isoplot 3.0 – a geochronological toolkit for Microsoft excel*. Berkley Geochron Center, Berkley, 70 p.
- Manninen, T., Pihlaja, P. & Huhma, H., 2001. U–Pb geochronology of the Peurasuvanto area, northern Finland. In: Vaasjoki, M. (ed.), *Radiometric age determinations from Finnish Lapland and their bearing on the timing of Precambrian volcano-sedimentary sequences*. Geological Survey of Finland, Special Paper 33, pp. 255–279.

- Mänttari, I., 1995. Lead isotope characteristics of epigenetic gold mineralization in the Palaeoproterozoic Lapland greenstone belt, northern Finland. *Geological Survey of Finland, Bulletin* 381, 70 p.
- Möller, A., O'Brien, P.J., Kennedy, A. & Kröner, A., 2002. Polyphase zircon in ultrahigh-temperature granulites (Rogaland, SW Norway): constraints for Pb diffusion in zircon. *Journal of metamorphic geology* 20, 727–740. <https://doi.org/10.1046/j.1525-1314.2002.00400.x>
- Nikkola, P., 2014. U–Pb zircon dating endeavors on the host rocks of the Juomasuo gold deposit, Kuusamo supracrustal belt, eastern Finland. MSc thesis, University of Helsinki, 57 p.
- Räsänen, J. & Huhma, H., 2001. U–Pb datings in the Sodankylä schist area, central Finnish Lapland. In: Vaasjoki, M. (ed.), *Radiometric age determinations from Finnish Lapland and their bearing on the timing of Precambrian volcano-sedimentary sequences*. Geological Survey of Finland, Special Paper 33, pp. 143–152.
- Räsänen, J. & Vaasjoki, M., 2001. The U–Pb age of a felsic gneiss in the Kuusamo schist area: reappraisal of local lithostratigraphy and possible regional correlations. In: Vaasjoki, M. (ed.), *Radiometric age determinations from Finnish Lapland and their bearing on the timing of Precambrian volcano-sedimentary sequences*. Geological Survey of Finland, Special Paper 33, pp. 143–152.
- Rosa, D.R.N., Finch, A.A., Andersen, T. & Inverno, C. M. C., 2009. U–Pb geochronology and Hf isotope ratios of magmatic zircon from the Iberian Pyrite Belt. *Mineralogy and Petrology* 95, 47–69. <https://doi.org/10.1007/s00710-008-0022-5>
- Schaltegger, U., Fanning, C.M., Günther, D., Maurin, J.C., Schulmann, K. & Gebauer, D., 1999. Growth, annealing and recrystallization of zircon and preservation of monazite in high-grade metamorphism: conventional and in-situ U–Pb isotope, cathodoluminescence and microchemical evidence. *Contributions to Mineralogy and Petrology* 134, 186–201. <https://doi.org/10.1007/s004100050478>
- Silvennoinen, A., 1972. On the stratigraphic and structural geology of the Rukatunturi area, northeastern Finland. *Geological Survey of Finland, Bulletin* 257, 48 p.
- Silvennoinen, A., 1991. Kuusamon ja Rukatunturin kartta-alueiden kallioperä. *Suomen geologinen kartta 1:100 000: kallioperäkarttojen selitykset lehdet 4524+4542, 4613*. Espoo: Geological tutkimuskeskus, 62 p. (In Finnish)
- Stacey, J.T. & Kramers, J.D., 1975. Approximation of terrestrial lead isotope evolution by a two-stage model. *Earth and Planetary Science Letters* 26, No. 2, 207–221. [https://doi.org/10.1016/0012-821X\(75\)90088-6](https://doi.org/10.1016/0012-821X(75)90088-6)
- Vanhanen, E.J., 2001. Geology, mineralogy and geochemistry of the Fe-Co-Au-(U) deposits in the Paleoproterozoic Kuusamo schist belt, Northeastern Finland. *Geological Survey of Finland, Bulletin* 399, 229 p.